Molecular Therapy
Nucleic Acids
Original Article

lncRNA ZEB1-AS1 Was Suppressed by p53 for Renal Fibrosis in Diabetic Nephropathy

Juan Wang,[1,2,4] Jian Pang,[1,2,4] Huiling Li,[3] Jie Long,[1] Fang Fang,[3] Junxiang Chen,[2] Xuejin Zhu,[2] Xudong Xiang,[1] and Dongshan Zhang[1,2]

[1]Department of Emergency Medicine, Second Xiangya Hospital, Central South University, Changsha, Hunan, China; [2]Department of Nephrology, Second Xiangya Hospital, Central South University, Changsha, Hunan, China; [3]Department of Ophthalmology, Second Xiangya Hospital, Central South University, Changsha, Hunan, China

The role of p53 in renal fibrosis is still controversial, and its underlying mechanisms remain not clear. Here, we showed that the pharmacological inhibition and genetic deletion of p53 in proximal tubular cells can attenuate renal dysfunction, tubular epithelial disruption, and interstitial fibrosis in db/db and STZ-induced diabetic nephrology (DN) mice. In human renal proximal tubule (human kidney 2 [HK-2]) cells, inhibition of p53 by PIF reduced the high glucose (HG)-induced extracellular matrix (ECM) accumulation and reversed the inhibitory effect of HG on mRNA expression levels of lncRNA zinc finger E-box binding homeobox1-antisense RNA 1 (ZEB1-AS1) and ZEB1. Interestingly, our results demonstrated that both lncRNA ZEB1-AS1 and ZEB1 exhibited an anti-fibrotic role, while ZEB1 is positively regulated by lncRNA ZEB1-AS1 during HG treatment. Mechanistically, lnc ZEB1-AS1 bound directly to H3K4 methyltransferase myeloid and lymphoid or mixed-lineage leukemia 1 (MLL1) and promoted H3K4me3 histone modification on ZEB1 promoter, which was reduced by HG treatment. ChIP analysis indicated the binding of p53 to the promoter region of lnc ZEB1-AS1. Furthermore, the findings were verified by the kidney biopsy samples from patients with DN. Taken all together, our results suggest that p53 may be a therapeutic target for renal fibrosis in DN.

INTRODUCTION

Diabetic nephropathy (DN), a major microvascular complication of diabetes, is characterized by the excessive accumulation of extracellular matrix (ECM) proteins in the renal tubulointerstitium, eventually leading to chronic renal failure.[1] Although the key pathogenic mechanisms underlying progressive DN have been identified, effective therapies remain elusive.[2]

p53 is a tumor suppressor gene. Previous studies have reported that the inhibition of p53 may ameliorate renal fibrosis induced by transforming growth factor beta (TGF-β), unilateral ureteral obstruction (UUO), and ischemia and reperfusion (I and R).[3–7] However, some studies found that genetic deletion and pharmacological inhibition of p53 may induce renal fibrosis in I and R and Alport syndrome (AS).[8,9] Therefore, the role of p53 in renal fibrosis remains controversial. Few studies suggested that p53 is responsible for the apoptosis of renal cell in DN.[10–12] In contrast, one study reported that p53 inhibition may decrease TGF-β-induced hypertrophy in mesangial cells (MMCs).[13] Hence, the regulatory mechanism of p53 in DN-induced renal fibrosis remains unclear. More recently, a study has found that gene knockout or pharmacological inhibition of p53 may prevent the development of diabetes by increasing the insulin secretion in streptozotocin (STZ)-induced type 1 and db/db type 2 diabetic mouse models.[14]

Long non-coding RNAs (lncRNA) are a novel class of non-protein-coding transcripts longer than 200 nt, which play a pivotal role in many diseases.[15–22] Recent studies have demonstrated that the antisense lncRNA is located in physical contiguity with zinc finger E-box binding homeobox 1 (ZEB1) and positively regulates the ZEB1 expression, which may contribute to the initiation or progression of tumors.[23,24] Moreover, it has been reported that ZEB1 suppressed the renal fibrosis induced by TGF-β1.[25] In light of this new evidence, we sought to determine whether p53 inhibition could ameliorate the renal fibrosis in DN via the inactivation of lncRNA ZEB1-antisense RNA1 (AS1) and ZEB1 pathway.

In the present study, we used proximal tubule-specific p53 knockout (PT-p53-KO) and pifithrin-α (PIF)-treated db/db mouse models to investigate the effects of p53 inhibition on renal fibrosis in DN. Additionally, we explored the molecular mechanisms underlying p53-induced renal fibrosis in DN, by targeting the expression of ZEB1 and lncRNA ZEB1-AS1.

RESULTS

p53 Is Induced in the Kidneys of db/db Diabetic Mice

Previous findings demonstrated that p53 is upregulated in the kidney tissues of STZ-induced diabetic mice at 4 weeks old.[12] In current

Received 24 April 2018; accepted 23 July 2018;
https://doi.org/10.1016/j.omtn.2018.07.012.

[4]These authors contributed equally to this work.

Correspondence: Dongshan Zhang, MD, Department of Emergency Medicine, Second Xiangya Hospital, Central South University, Changsha, Hunan 410011, China.
E-mail: 715653110@qq.com
Correspondence: Xudong Xiang, MD, Department of Emergency Medicine, Second Xiangya Hospital, Central South University, Changsha, Hunan 410011, China.
E-mail: xudongx_99@hotmail.com

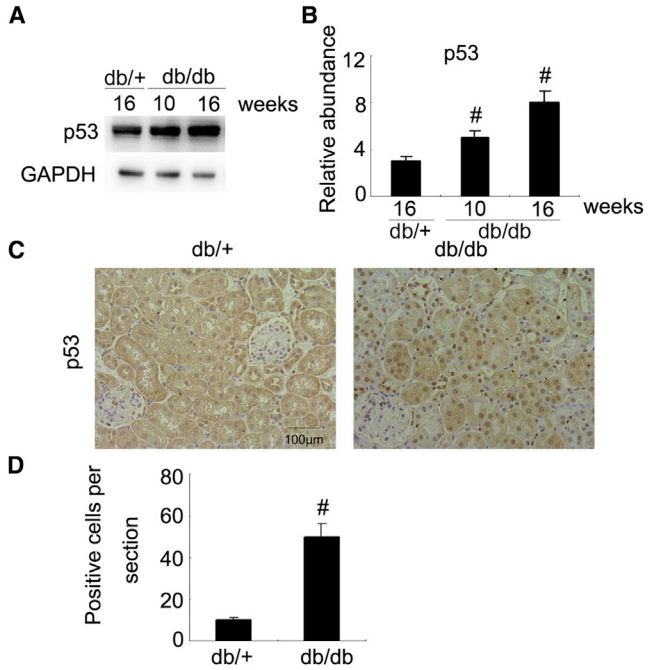

Figure 1. Induction of p53 in the Kidney of db/db Diabetic Mice

(A) Immunoblot analysis of p53 and GAPDH (loading control) in mouse kidneys of db/db groups at the indicated time points. (B) Densitometric analysis is performed on each group (n = 8). (C) Immunohistochemical staining of p53 in the kidney of db/+ or db/db diabetic mice at week 16. (D) Quantification of p53 staining. Original magnification, ×200. Bar, 100 μm. Data are expressed as means ± SD (n = 8). #p < 0.05, mice at weeks 10 and 16 versus db/+ mice.

study, we found that the expression of p53 was low in db/+ mice but gradually increased in db/db mice at weeks 10 and 16 (Figures 1A and 1B). The immunohistochemical results showed that p53 was mainly enriched in the renal tubular cells of db/db mice at week 16 (Figures 1C and 1D). These data support that p53 is associated with the progression of DN in db/db mice.

PIF Ameliorates Renal Dysfunction and Fibrosis in db/db Diabetic Mice

A recent study reported that the pre-treatment of PIF can prevent the occurrences of diabetes in 6-week-old db/db mice.[14] However, the effect of post-treatment of PIF on the progression of diabetics in db/db mice remains unclear. The ten-week-old db/db diabetic mice were used in present study. After 6 weeks, the db/db diabetic mice indicated the higher levels of blood glucose, serum creatinine, and urinary albumin-to-creatinine ratio (ACR) but lower body weight, which was markedly reversed by PIF treatment (Figures 2A, 2C, and 2D). In surprise, the PIF treatment did not affect the blood glucose level in db/db diabetic mice (Figure 2B). Both the histology and Masson trichrome staining showed the obvious tubular epithelial disruption, hypertrophy of glomeruli, and renal fibrosis in db/db diabetic mice, which, except for hypertrophy of glomeruli, was also attenuated by PIF treatment (Figures 2E–2H).

PIF Reduces ECM Accumulation in db/db Diabetic Mice

In order to verify the amelioration of renal fibrosis by PIF treatment, the immunoblotting technique was used. The results indicated that the expression levels of collagen I, collagen IV, fibronectin, α-SMA, and p53 were markedly increased in db/db diabetic mice, which can be suppressed by PIF treatment (Figures 3A and 3B). These findings were confirmed by immunohistochemical staining of the same proteins (Figures 4A and 4B).

p53 Deletion Attenuates Renal Dysfunction and Fibrosis in STZ-Induced DN Mice

To further confirm these findings, we investigated whether p53 knockout from proximal tubules can attenuate STZ-induced kidney injury. The male wild-type (PT-p53-WT) and PT-p53-KO littermate mice were injected with STZ to induce diabetes. After 8 weeks, their body weights, blood glucose, serum creatinine, and albumin and creatinine ratio (ACR) were detected. As compared to STZ-treated PT-p53-WT mice, STZ-treated PT-p53-WT group exhibited higher levels of blood glucose, serum creatinine, and urinary ACR, but lower body weight. These markers were significantly reversed in PT-p53-KO mice treated with STZ, except for blood glucose levels (Figures 5A–5D). In STZ-treated PT-p53-KO group, tubular epithelial disruption and renal fibrosis, but not glomerular hypertrophy, were markedly ameliorated (Figures 5E–5H).

p53 Deletion Reduces ECM Accumulation in STZ-Induced DN Mice

To further confirm the results of Masson trichrome staining, the expressions of collagen I, collagen IV, fibronectin, and α-SMA were detected with immunoblotting. The expressions of these protein markers were markedly increased in STZ-PT-p53-WT group as compared to non-treated PT-p53-WT group, while significantly reduced in STZ-treated PT-p53-KO group (Figures 6A and 6B). Notably, p53 expression was lower in the kidney tissues of PT-p53-KO than of PT-p53-WT, suggesting p53 ablation in knockout mice (Figures 6A and 6B). In addition, the immunohistochemical staining demonstrated similar results (Figures 7A and 7B). Furthermore, pH3 ser10 has been considered as a hallmark of G2 and M arrest and profibrotic phenotype. The results of immunohistochemical staining indicated that the expression of pH3 ser10 was significantly higher in STZ-treated PT-p53-WT mice than the non-treated PT-p53-WT mice, while significantly reduced in STZ-treated PT-p53-KO mice. The findings of immunohistochemical staining were verified by western blot results (Figures 7C and 7D), suggesting that p53 inhibition may attenuate STZ-induced DN, at least partly through the modulation of G2 and M arrest.

PIF Treatment Attenuates HG-Induced ECM Accumulation in HK-2 Cells

A previous study reported that high glucose (HG) induced p53 accumulation in the rat kidney proximal tubular cells (RPTC).[12] In the present study, we observed that HG may induce the

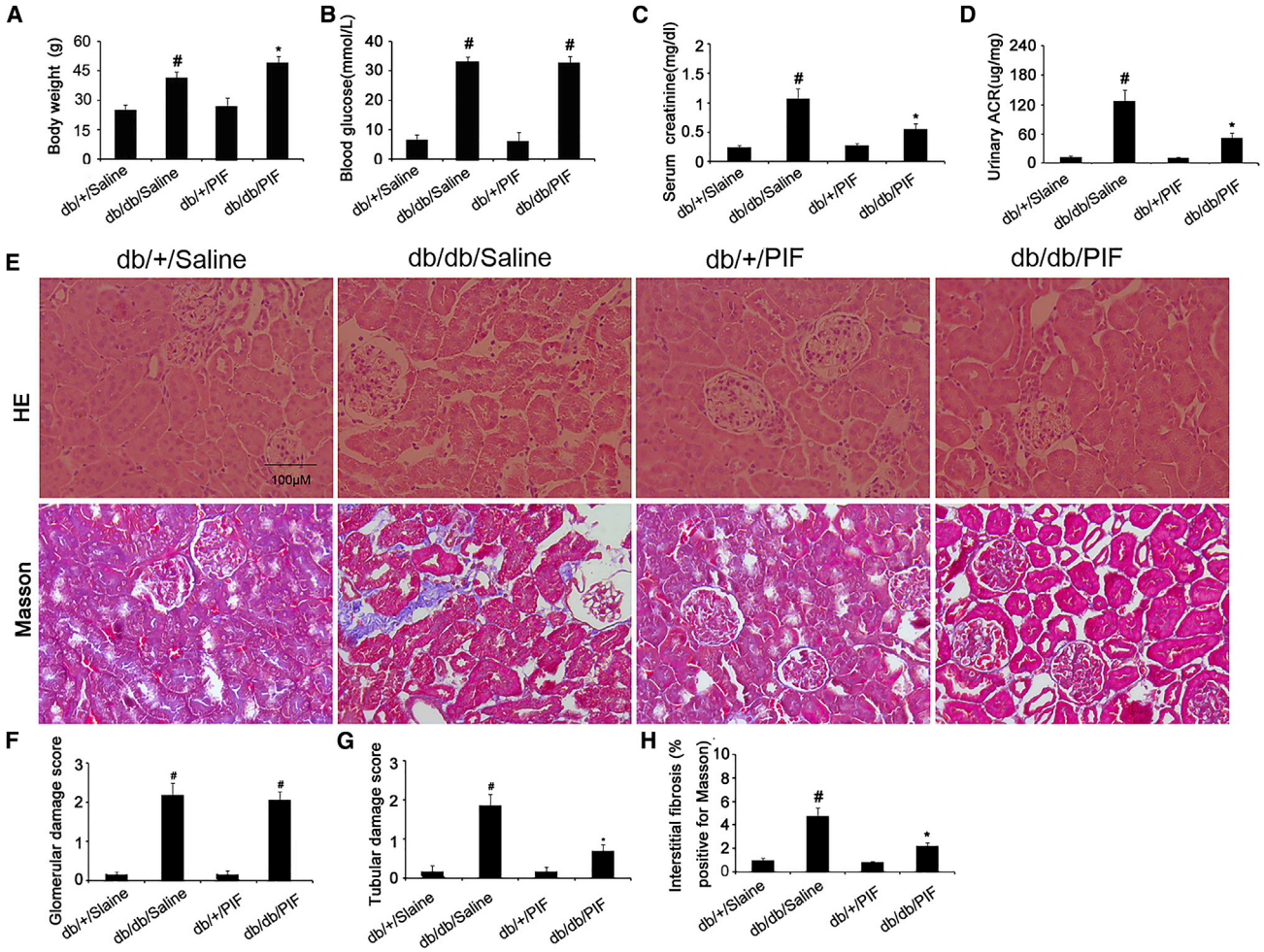

Figure 2. Attenuation of Renal Fibrosis by PIF Treatment

The body weights of the mice (A). Blood and urine samples are collected for glucose (B), serum creatinine (C), and urinary ACR (D) measurements. Renal cortical tissues are collected for H&E staining and Masson staining (E), quantification of glomerular damage score (F), tubular damage score (G), and tubulointerstitial fibrosis (H) in the kidney cortex. Original magnification, ×200. Bar, 100 μm. Data are expressed as means ± SD (n = 8). #$p < 0.05$, saline-treated db/db group versus saline-treated db/+ group; *$p < 0.05$, PIF-treated db/db group versus saline-treated db/db group.

accumulation of p53, vimentin, collagen I, collagen IV, and fibronectin in HK-2 cells at different time points (Figures 8A and 8B). To investigate the role of p53 in HG-induced renal fibrosis, PIF, the small-molecule inhibitor of p53 transcriptional activity, was used in this study. Interestingly, we found that HG treatment markedly increased the expression of p53 and the accumulation of ECM proteins but significantly suppressed by PIF treatment (Figures 8C and 8D). These findings are consistent with the *in vivo* results, in which p53 plays a pivotal role in STZ- or db/db mutation-induced DN.

lnc ZEB1-AS1 Knockdown Increases HG-Induced ECM Accumulation via the Inhibition of ZEB1

To elucidate the molecular mechanisms underlying p53-induced renal fibrosis, we focused on the expression of lncRNA following renal fibrosis.[26–29] Recent studies demonstrated that lnc ZEB1-AS1 may activate ZEB1 expression in cancer tissues and cell lines,[24,30] while ZEB1 may suppress the excessive accumulation of ECM proteins in DN.[25,31] Thus, we hypothesized that lnc ZEB1-AS1 may protect against HG-induced renal fibrosis. The results of real-time PCR demonstrated that the expression of lnc ZEB1-AS1 was significantly suppressed by HG at 24 hr, 48 hr, and 72 hr (Figure S1A). Interestingly, the expression of ZEB1 showed a similar trend with lnc ZEB1-AS1 expression (Figures S1B and S1C), supporting the findings from tumor cell lines.[24,30] After transfection of siRNA ZEB1-AS1 for 72 hr, the expression of lnc ZEB1-AS1 was further suppressed in HG treatment group (Figure S1D). Additionally, our results indicated that HG treatment markedly increased the expressions of vimentin, collagen I, collagen IV, and fibronectin but suppressed ZEB1 expression. However, these changes can be

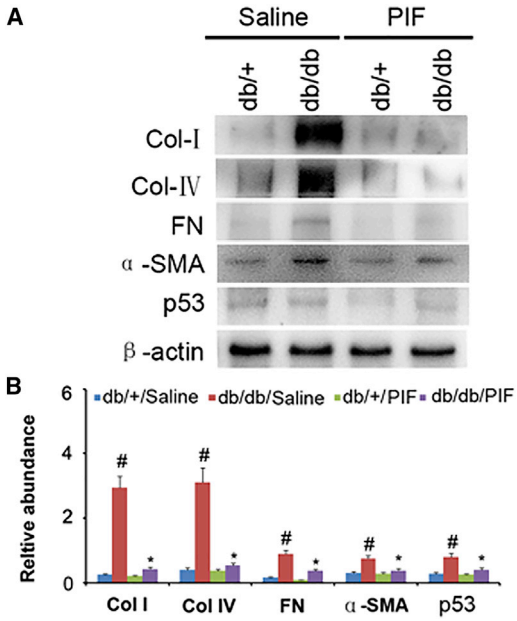

Figure 3. PIF Treatment Inhibited the Expressions of Collagen I, Collagen IV, Fibronectin, α-SMA, and p53 Detected by Immunoblotting

(A) Western blot analysis of collagen I, collagen IV, fibronectin, α-SMA, p53, and β-actin by using the specific antibodies. (B) Densitometric quantification of western blot bands. Data are expressed as means ± SD (n = 8). #p < 0.05, saline-treated db/db group versus saline-treated db/+ group; *p < 0.05; PIF-treated db/db group versus saline-treated db/db group.

reversed by the transfection of small interfering RNA (siRNA) ZEB1-AS1 (Figures S1E and S1F). Taken together, the inhibition of lnc ZEB1-AS1 may increase HG-induced ECM accumulation by downregulating ZEB1 expression.

lnc ZEB1-AS1 Binds to H3K4 Methyltransferase MLL1 and Promotes H3K4me3 Histone Modification in ZEB1 Promoter

To investigate the regulation of lnc ZEB1-AS1 on ZEB1 expression, RIP assays were performed. We demonstrated that the degree of lnc ZEB1-AS1 bound to myeloid and lymphoid or mixed-lineage leukemia 1 (MLL1) was higher than MLL2 and MLL3 in HK-2 cells (Figure S2A). In addition, chromatin immunoprecipitation (ChIP) assays revealed that the levels of MLL2 and MLL3 were lower at the promoter of ZEB1 as compared to MLL1 (Figure S2B). Furthermore, H3K4me3 can directly bind to the promoter of ZEB1, but not H3K4me2, H3K4me1, and H3K4 (Figure S2C). Both MLL1 occupancy and H3K4me3 binding at ZEB1 promoter were reduced by the knockdown of lnc ZEB1-AS1 and the treatment of HG in HK-2 cells (Figures S2D and S2E).

p53 Suppresses the Expression of lnc ZEB1-AS1 via the Physical Interaction with Its Promoter Region

lnc ZEB1-AS1 plays an important role in HG-induced ECM accumulation; however, it remains unclear whether p53 can regulate the expression of lnc ZEB1-AS1. Our results demonstrated that HG treatment markedly suppressed the expression levels of lnc ZEB1-AS1 and ZEB1, which can be reversed by PIF treatment (Figures S3A–S3C). In addition, ChIP assay was used to determine the interaction between p53 and lnc ZEB1-AS1 promoter region in HK-2 cells. As shown in Figure S3D, the antibody directed against p53 may immunoprecipitate the DNA fragments containing the potential binding sites of p53 binding site (pBS1) and pBS2. These findings support the hypothesis that the physical interaction between p53 and lnc ZEB1-AS1 promoter in HG group is stronger than that in normal glucose group. Furthermore, p53 suppressed the expression of lnc ZEB1-AS1 to downregulate ZEB1 during renal fibrosis.

The Expressions of p53 and lnc ZEB1-AS1 and ZEB1 Signaling and ECM-Related Genes in Human Diabetic Kidneys

In order to extend the results of the *in vitro* study, the renal expressions of p53, lnc ZEB1-AS1, ZEB1, and ECM-related genes were examined in DN patients. The kidneys of DN patients demonstrated glomerular damage and tubulointerstitial injury or fibrosis compared to the kidneys from patients with minimal change disease (MCD) (nc = c8 in each group). Moreover the expression levels of p53, collagen I, collagen IV, fibronectin, and α-SMA were higher in DN patients than in MCD patients (Figure S4A). However, the expression level of ZEB1 was decreased in DN patients, as consistent with the expression of lnc ZEB1-AS1 (Figure S4I). The semiquantitative scoring of immunostaining data further confirmed the above findings, as shown in Figures S4B–S4H. Collectively, these results indicate that p53 and lnc ZEB1-AS1 and ZEB1 signaling may be involved in human DN.

DISCUSSION

The pathologic role of p53 in renal fibrosis remains controversial. This study reported for the first time that p53 inhibitors and proximal tubular knockout of p53 can ameliorate the interstitial fibrosis in db/db mice and STZ-induced DN mice, respectively. More importantly, the present study revealed that p53 may decrease ZEB1 expression to promote renal fibrosis in HK-2 cells via the direct downregulation of lnc ZEB1-AS1. In addition, we detected the consistent changes of these molecules in human DN samples. All together, our findings provide new insights into the mechanisms underlying p53-induced renal fibrosis in DN.

In the current study, we demonstrated that p53 is primarily expressed in renal tubular cells of db/db mice, but not glomerular cells. Furthermore, PIF treatment ameliorated renal dysfunction, tubular epithelial disruption, and renal fibrosis in db/db mice, except for glomerular hypertrophy. Hoshino et al.[14] have reported that PIF-inhibited p53 can enhance glucose intolerance in db/db mice. However, our results showed that PIF does not influence the degree of hyperglycemia at the indicated time points, suggesting that the effect of PIF treatment in DN is accompanied by hypoglycemia. The divergence of results can be further explained by different PIF dosage (3 mg•kg-1 versus 1.1 mg•kg-1) and treatment duration (6 weeks versus 10 weeks) between our study and Hoshino

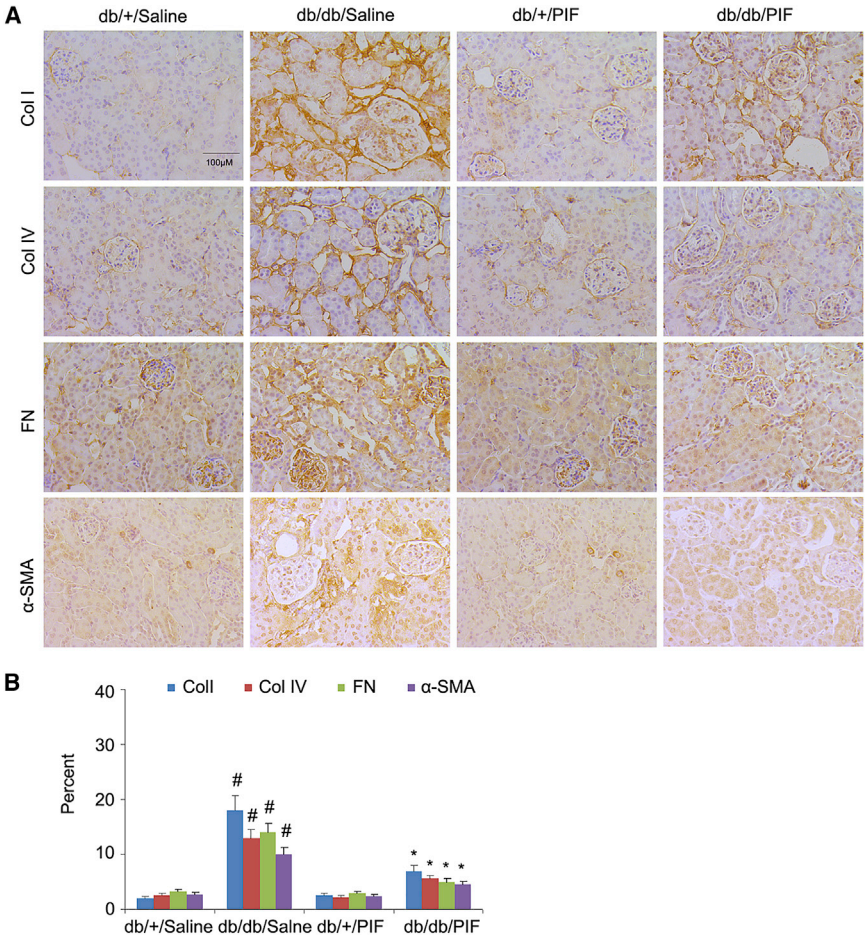

Figure 4. PIF Treatment Suppressed the Expressions of Collagen I, Collagen IV, Fibronectin, α-SMA, and p53 Detected by Immunohistochemistry

(A) The expressions of collagen I, collagen IV, fibronectin, and α-SMA were analyzed by immunohistochemical staining (B). Original magnification, ×200. Bar, 100 μm. Data are expressed as means ± SD (n = 8). #$p < 0.05$, saline-treated db/db group versus saline-treated db/+ group; *$p < 0.05$, PIF-treated db/db group versus saline-treated db/db group.

et al.,[14] indicating that PIF pre-treatment but not post-treatment may prevent the occurrence of diabetes.

To further confirm the role of p53 in DN, targeted deletion of p53 in proximal tubular was applied, since p53 global knockout mice have been reported to protect against the development of diabetes by preventing β-cell mitochondrial dysfunction.[14] Nevertheless, p53 deletion may attenuate renal dysfunction, tubular epithelial disruption, and renal fibrosis in STZ-induced DN mice, which is consistent with the outcome of PIF treatment in db/db mice. Despite these promising results, the degree of hyperglycemia was relatively similar between PT-p53-WT and PT-p53-KO mice, suggesting that deletion of p53 in tubular cells is not sufficient to affect the progression of STZ-induced diabetes.

To further investigate the mechanisms of p53 anti-fibrosis on diabetic nephrology, we focus on the lnc ZEB1-AS1. The inhibition of it aggravated the HG-induced ECM accumulation, which suggested that lnc ZEB1-AS1 could be considered as an anti-fibrosis lncRNA (Figure S1). Although some studies demonstrated that lnc ZEB1-AS1 might activate ZEB1 in tumor cell lines,[24,30] their interaction remains unclear in HK-2 cells. In the current study, we observed that lnc ZEB1-AS1 positively regulates the expression of ZEB1 in HK-2 cells. Several studies have demonstrated that the genetic deletion of ZEB1 and ZEB2 (another Zeb family gene) in mice can lead to renal fibrosis *in vitro* and kidney disease, respectively.[25,32] Hence, we postulated that HG induces renal fibrosis by downregulating lnc ZEB1-AS1 to suppress ZEB1 expression.

A previous study has demonstrated that lnc ZEB1-AS1 directly binds and recruits MLL1 to ZEB1 promoter in tumor cell lines.[24] However, little is known about the other family genes such as MLL2 and MLL3. In the current study, we found that MLL2 and MLL3 exhibit similar function as MLL1, but their capability of binding is much lower than MLL1 (Figures S2A and S2B), supporting the major role of MML1 during transcription process. In addition, we observed that only H3K4me3 can bind directly to the promoter region of ZEB1 (Figure S2C). Furthermore, MLL1 and H3K4me3 bind with ZEB1 to attenuate the knock down of lnc ZEB1-AS1 and HG treatment conditions (Figures S2D and S2E). Interestingly, the results indicated that the reduced expressions of lnc ZEB1-AS1 and ZEB1 can be reversed by PIF treatment in HG-treated cells (Figure S3), supporting that p53 negatively regulates their expression levels. Furthermore, by using ChIP assays, we demonstrated for the first time that p53 could physically interact with the promoter region of lnc ZEB1-AS1 (Figure S3). Collectively, these data suggest a novel regulatory mechanism by which p53 directly reduced lnc ZEB1-AS1 to suppress ZEB1 in HK-2 cells (Figure S5). This mechanism seems to be true not only in HK-2 cells, but also in fibrotic kidney samples collected from DN patients (Figure S4). There is, however, a clear limitation that lnc ZEB1-AS1 expression has not been detected in DN mouse model, due to its highly conservative sequences.

In this study, we demonstrate that p53 is associated with renal interstitial fibrosis in DN, as evidenced by the amelioration of renal fibrosis by p53 inhibitors and p53 gene deletion. Moreover, p53 inhibition may induce the expression of ZEB1 through upregulation of lnc

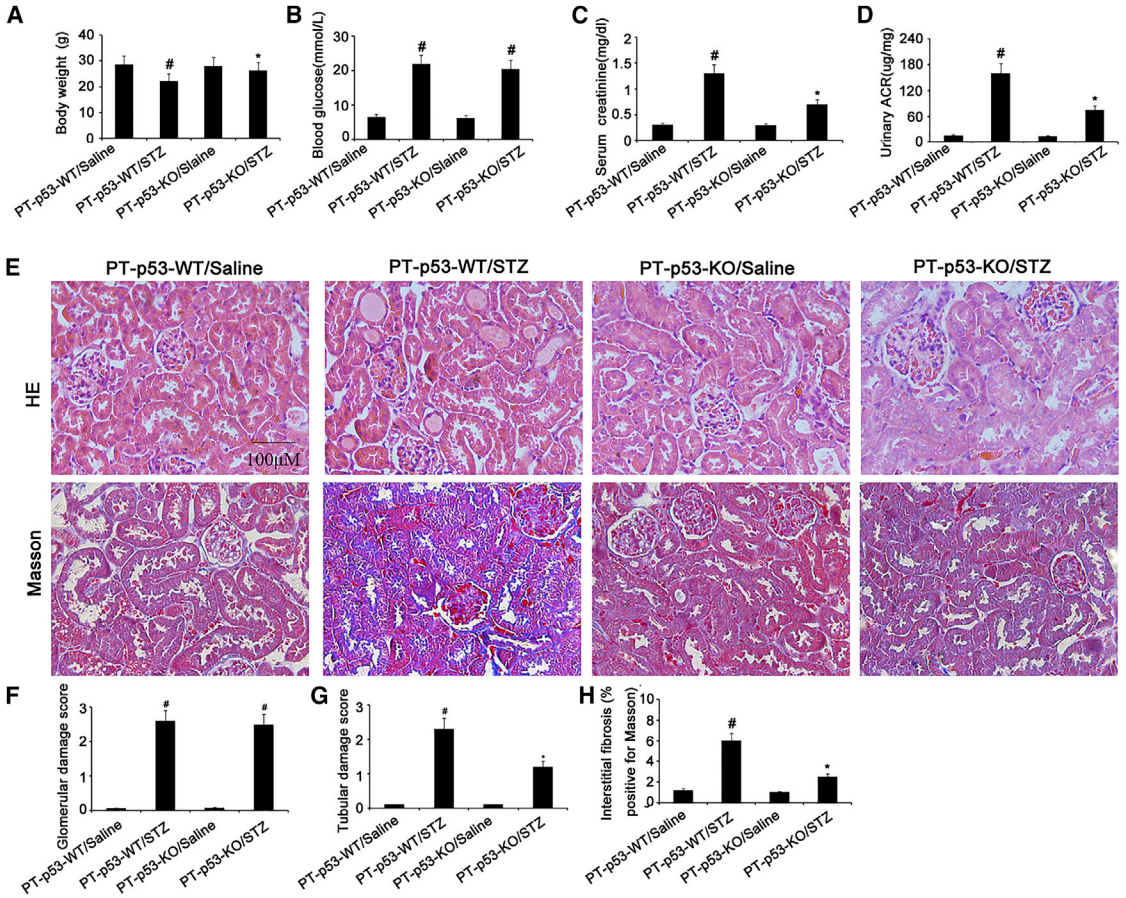

Figure 5. Amelioration of Renal Fibrosis following p53 Deletion

The body weights of the mice (A). Blood and urine samples are collected for glucose (B), serum creatinine (C), and urinary ACR (D) measurements. Renal cortical tissues are collected for H&E staining and Masson staining (E), quantification of glomerular damage score (F), tubular damage score (G), and tubulointerstitial fibrosis (H) in the kidney cortex. Original magnification, ×200. Bar, 100 μm. Data are expressed as means ± SD (n = 8). #p < 0.05, STZ-treated PT-p53-WT group versus saline-treated PT-p53-WT group; *p < 0.05, STZ-treated PT-p53-KO group versus saline-treated PT-p53-KO group.

ZEB1-AS1. In addition, we provide evidence that p53 and lnc ZEB1-AS1 and ZEB1 axis may be associated with renal fibrosis in human DN. Taken all together, these findings suggest that p53 may be a potential therapeutic target for renal fibrosis in DN.

MATERIALS AND METHODS

Antibodies and Reagents

Antibodies of anti-GAPDH, anti-β-actin, anti-collagen I, anti-collagen IV, anti-vimentin, anti-α-SMA, and anti-fibronectin were obtained from Santa Cruz Biotechnology (Santa Cruz, CA, USA). Meanwhile, anti-p53, MLL1, MLL2, MLL3, H3K4me3, H3K4me2, H3K4me1, H3K4, and ZEB1 were purchased from Cell Signaling Technology (Danvers, MA, USA). All the secondary antibodies were obtained from Thermo Fisher Scientific (Waltham, MA, USA). The recombinant human TGF-β1 was purchased from R&D Systems (Minneapolis, MN, USA). Moreover, PIF and STZ were obtained from Sigma-Aldrich (Shanghai, China).

Animals

The C57BL6/KsJ-leprdb (db/db) and WT control C57 (+/+) mice were obtained from Shanghai Animal Center (Shanghai, People's Republic of China). Proximal tubule-specific p53-deletion mice were generated by crossing phosphoenolpyruvate carboxykinase-cyclization recombination (PEPCK-Cre) mice with p53 (flox/flox) mice (Jackson Laboratory) as described previously.[3,30] Animal experiments were conducted in accordance with the guidelines established by the Animal Care Ethics Committee of Second Xiangya Hospital, People's Republic of China. After we obtained ethics approval, the mice were housed in a 12-hour light/dark cycle with *ad libitum* access to food and water.

Human Samples

The research protocol was approved by the Hospital Review Board. Archival human kidney biopsy samples were collected from patients with DN (n = 8) and MCD (n = 8) at the Second Xiangya Hospital, People's Republic of China. Written informed consent was obtained

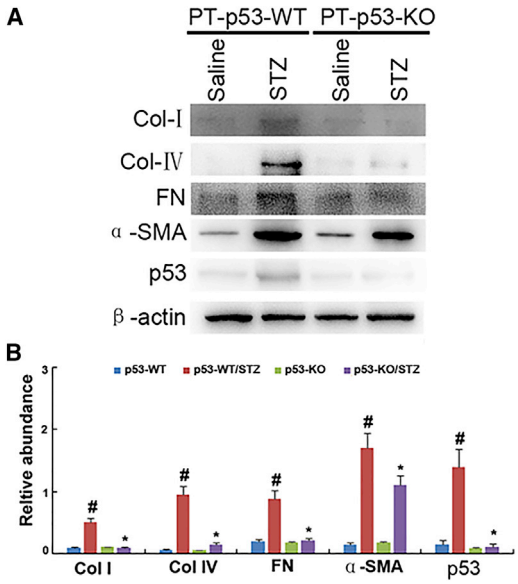

Figure 6. Inhibition of Collagen I, Collagen IV, Fibronectin, α-SMA, and p53 Expressions Analyzed by Immunoblotting following p53 Deletion

(A) Western blot analysis of collagen I, collagen IV, fibronectin, α-SMA, p53, and β-actin by using specific antibodies. (B) Densitometric quantification of western blot bands. Data are expressed as means ± SD (n = 8). #p < 0.05, STZ-treated PT-p53-WT group versus saline-treated PT-p53-WT group; *p < 0.05, STZ-treated PT-p53-KO group versus saline-treated PT-p53-KO group.

from all participants. Some of the specimens were fixed with 4% buffered paraformaldehyde, while the remaining samples were soaked in RNA later solution (Ambion) and stored at −80°C until use.

Animal Models

For the STZ induction of diabetes, PT-p53-WT and PT-p53-KO littermate mice at 8 weeks of age were injected with 50 mg/kg body weight STZ for 5 consecutive days.[12] The homozygous db/db and WT (10 weeks old) mice were administered intraperitoneally with PIF at a dose of 3 mg/kg three times weekly for 6 weeks. Fasting blood glucose levels of more than 200 mg/dL for two consecutive readings were considered diabetic.

Cell Culture and Treatments

HK-2 cells were cultured in DMEM (Sigma-Aldrich) supplemented with 10% fetal bovine serum and 0.5% penicillin and streptomycin. Cultures were maintained at 37°C in a humidified atmosphere of 5% CO_2. Subsequently, HK-2 cells were treated with or without PIF (10 μM) or 5–30 mM D-glucose or mannitol. For gene disruption, the cells were incubated with siRNA ZEB1-AS1 or ZEB1 (100 nM) or negative control (siR-neg; Sigma-Aldrich).

Analysis of Renal Function and Physiological Parameters

The body weights and blood glucose levels of mice were measured. BCG (Bromocresol Green) albumin assay kit was used to detect the levels of urine albumin. Serum and urine creatinine levels were analyzed using the high-performance liquid chromatography (HPLC) method.[33] The ACR was calculated using the method described previously.[34]

Histology, Immunohistochemistry, and Immunoblot Analyses

Kidney tissues were fixed in 4% buffered paraformaldehyde, embedded in paraffin. All sections (4 μm in thickness) were stained with H&E and Masson's trichrome.[3,35] Immunohistochemical analysis was performed using anti-α-SMA, anti-collagen I, anti-fibronectin, and anti-collagen IV, according to the previous protocol.[36–38] For the quantitation step, the detailed procedures have been described in our recent work.[37] For immunoblot analysis, lysates from HK-2 cells or kidneys were extracted by using SDS polyacrylamide electrophoresis (Sigma-Aldrich) with phosphatase inhibitors (Calbiochem). Western blotting and antibody exposure were performed according to standard procedures.

Real-Time PCR Analysis of lncRNA-ZEB1-AS1

Total RNA was extracted from kidney cortical tissues and HK-2 cells by using Trizol Reagent (Invitrogen, Carlsbad, CA, USA) according to the manufacturer's instructions. Approximately 40 ng of total RNA was reverse-transcribed using M-MLV Reverse Transcriptase (Invitrogen). Real-time qPCR was performed by using Bio-Rad (Hercules, CA) IQ SYBR Green Supermix with Opticon (MJ Research, Waltham, MA, USA) according to the manufacturer's protocols. The sequences of lncRNA-ZEB1-AS1 and ZEB1 were retrieved from GenBank database (gen ID, 220930 and 6935, respectively). The expression of target gene was normalized against GAPDH. The primers used are as follows: ZEB1-AS1, 5′-CCGTGGGCACTGCTGAAT-3′ (forward) and 5′-CTGCTGGCAAGCGGAACT-3′ (reverse); ZEB1, 5′-ACTCTG ATTCTACACCGC-3′ (forward) and 5′-TGTCAC ATTGATA GGGCTT-3′ (reverse); and GAPDH, 5′-GGTCTCCTCTGACTT CAAC A-3′ (forward) and 5′-GTGAGGGTCTCTCTCTTCCT-3′ (reverse). Quantification was done using ΔCt values.

RNA Immunoprecipitation

Cells were pelleted and lysed. RNA immunoprecipitation (RIP) was carried out according to the manufacturer's protocols. RNA fragments were purified, digested with DNase, and used as a template for qRT-PCR.[19] The primers for ZEB1-AS1 were 5′-TCCCT GCTAAGCTT CCTTCAGTGT-3′ and 5′- GACAGTGATCACTTT CATA TCC-3′.

ChIP Analysis

ChIP was performed as described previously[3,39] with primary antibodies against p53. Precipitated DNAs were detected by PCR using specific primers pBS1, 5′-TTACAGTTCCATGCAGTGTCT-3′ and 5′-GTCTCGAACTCCTGACCTCA-3′; pBS2, 5′-GTCAGGGACCA TATTAGGCATT-3′, and 5′- CTTGGCCTCTCAAAG TGCTG-3′; and with anti-H3K4me3 antibody (rabbit monoclonal; Merck Millipore) or rabbit non-immune immunoglobulin G (IgG) (as negative control). The specific primers used for the promoter fragment

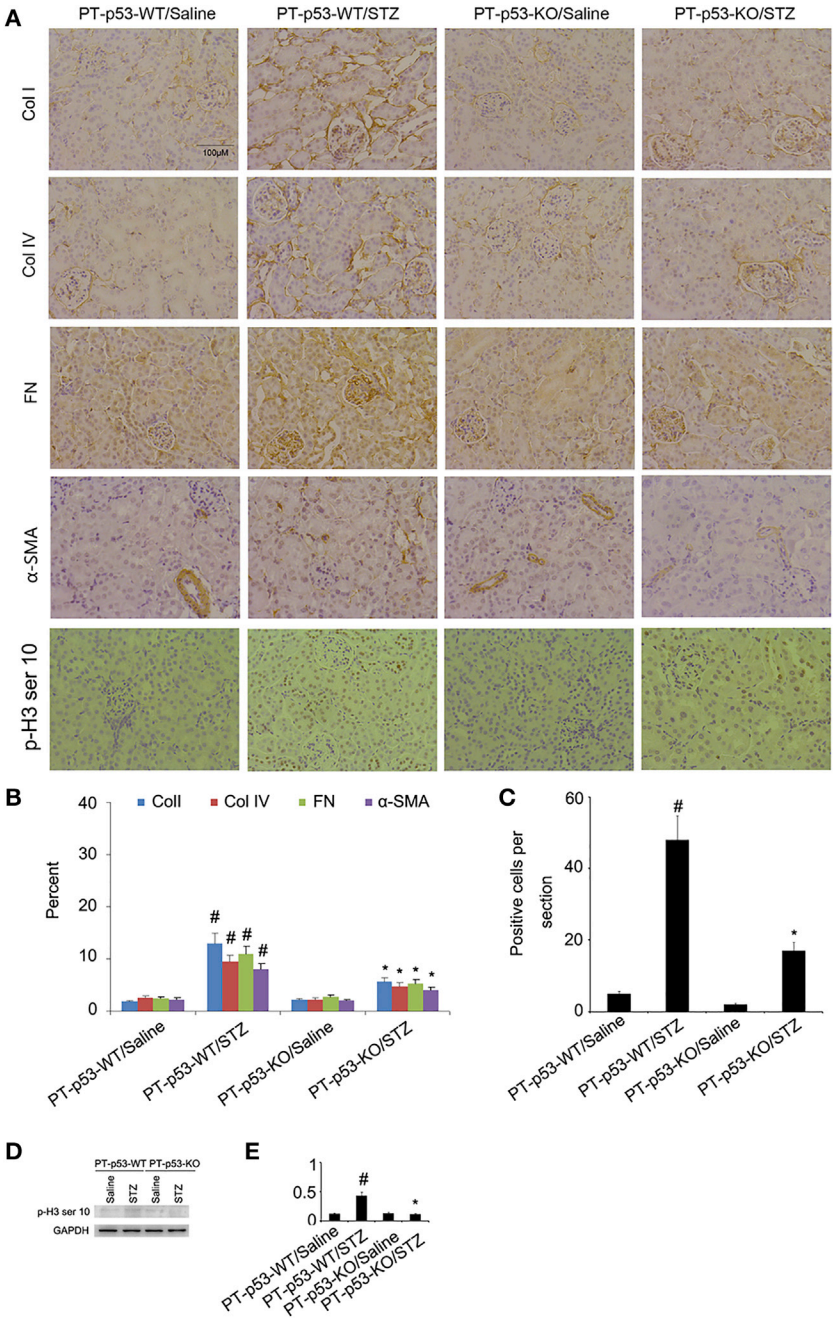

Figure 7. Suppression of Collagen I, Collagen IV, Fibronectin, and α-SMA Expressions Analyzed by Immunochemistry following p53 Deletion

(A) The expressions of collagen I, collagen IV, fibronectin, α-SMA, and pH3 ser10 analyzed by immunohistochemical staining. (B and C) Quantification of immunohistochemical staining of collagen I, collagen IV, fibronectin, and α-SMA (B) and ph3 ser10 (C). (D) Representative immunoblots of pH3 ser10 and GAPDH. (E) Densitometric measurement of pH3 ser10 protein signal. Original magnification, ×200. Bar, 100 μm. Data are expressed as means ± SD (n = 8). #p < 0.05, STZ-treated PT-p53-WT group versus saline-treated PT-p53-WT group; *p < 0.05, STZ-treated PT-p53-KO group versus saline-treated PT-p53-KO group.

of ZEB1 (ZEB1-pro) were 5′-CGTAGAGCGAGAGCCTCTAGG TGTAAG-3′ and 5′-CCTCTCGCTTGTGTCTAAATGC TCGAG-3′.

Statistical Analyses

Quantitative data are expressed as means ± SDs. Statistical analysis was conducted using the GraphPad Prism software. Multiple groups were compared by use of one-way ANOVA followed by Tukey's post-tests. Two-tailed unpaired or paired t tests were used to compare the differences of two groups. $p < 0.05$ was considered significantly different.

Accession Numbers

The sequences of lncRNA-AS1 and ZEB1 were retrieved from GenBank database (https://www. https://www.ncbi.nlm.nih.gov/gene/?term=220930, and https://www.ncbi.nlm.nih.gov/gene/?term=6935, respectively).

SUPPLEMENTAL INFORMATION

Supplemental Information includes five figures and can be found with this article online at https://doi.org/10.1016/j.omtn.2018.07.012.

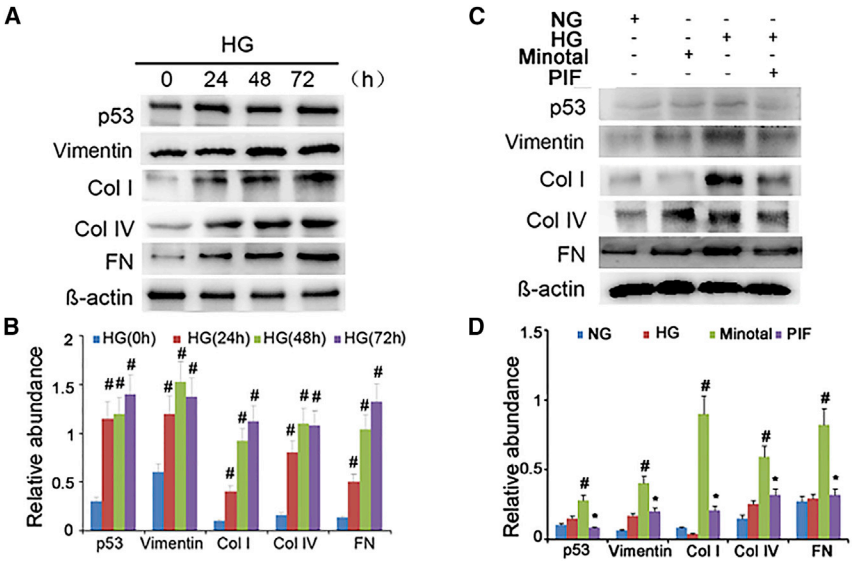

Figure 8. PIF Suppressed collagen I, Collagen IV, Fibronectin, Vimentin, and High-Glucose-Induced p53 Expressions

(A) Western blot analysis of p53, collagen I, collagen IV, fibronectin, and vimentin at the indicated time points. (B) Densitometric quantification of western blot bands. (C) Relative protein expression levels of p53, collagen I, collagen IV, fibronectin, vimentin, and β-actin at 24 hr after PIF treatment coupled with or without HG. (D) Densitometric measurements of western blot bands. Data are expressed as means ± SD (n = 6). #$p < 0.05$, 48 hr or 72 hr versus 0 hr or 24 hr, and HG group versus normal glucose group; *$p < 0.05$, HG+PIF group versus HG group.

AUTHOR CONTRIBUTIONS

D.Z. and X.X. conceived and designed the experiments; J.W., J.P., and H.L. carried out the experiments; H.L., F.F., J.C., J.L., and X.Z. analyzed the data; X.X. and H.L. contributed reagents, materials, and analysis tools; D.Z. wrote the main manuscript text, but all authors reviewed the manuscript.

CONFLICTS OF INTEREST

We declare that we have no conflicts of interest.

ACKNOWLEDGMENTS

The study was supported in part by a grant from the National Natural Science Foundation of China (81570646 and 81500756) and the Excellent Youth Foundation of Hu'nan Scientific Committee (2017JJ1035).

REFERENCES

1. Loeffler, I., and Wolf, G. (2015). Epithelial-to-Mesenchymal Transition in Diabetic Nephropathy: Fact or Fiction? Cells *4*, 631–652.

2. Zeisberg, M., and Neilson, E.G. (2010). Mechanisms of tubulointerstitial fibrosis. J. Am. Soc. Nephrol. *21*, 1819–1834.

3. Yang, R., Xu, X., Li, H., Chen, J., Xiang, X., Dong, Z., and Zhang, D. (2017). p53 induces miR199a-3p to suppress SOCS7 for STAT3 activation and renal fibrosis in UUO. Sci. Rep. *7*, 43409.

4. Yang, L., Besschetnova, T.Y., Brooks, C.R., Shah, J.V., and Bonventre, J.V. (2010). Epithelial cell cycle arrest in G2/M mediates kidney fibrosis after injury. Nat. Med. *16*, 535–543, 1p following 143.

5. Overstreet, J.M., Samarakoon, R., Meldrum, K.K., and Higgins, P.J. (2014). Redox control of p53 in the transcriptional regulation of TGF-β1 target genes through SMAD cooperativity. Cell. Signal. *26*, 1427–1436.

6. Samarakoon, R., Dobberfuhl, A.D., Cooley, C., Overstreet, J.M., Patel, S., Goldschmeding, R., Meldrum, K.K., and Higgins, P.J. (2013). Induction of renal fibrotic genes by TGF-β1 requires EGFR activation, p53 and reactive oxygen species. Cell. Signal. *25*, 2198–2209.

7. Ying, Y., Kim, J., Westphal, S.N., Long, K.E., and Padanilam, B.J. (2014). Targeted deletion of p53 in the proximal tubule prevents ischemic renal injury. J. Am. Soc. Nephrol. *25*, 2707–2716.

8. Dagher, P.C., Mai, E.M., Hato, T., Lee, S.Y., Anderson, M.D., Karozos, S.C., Mang, H.E., Knipe, N.L., Plotkin, Z., and Sutton, T.A. (2012). The p53 inhibitor pifithrin-α can stimulate fibrosis in a rat model of ischemic acute kidney injury. Am. J. Physiol. Renal Physiol. *302*, F284–F291.

9. Fukuda, R., Suico, M.A., Kai, Y., Omachi, K., Motomura, K., Koga, T., Komohara, Y., Koyama, K., Yokota, T., Taura, M., et al. (2016). Podocyte p53 Limits the Severity of Experimental Alport Syndrome. J. Am. Soc. Nephrol. *27*, 144–157.

10. Jung, D.S., Lee, S.H., Kwak, S.J., Li, J.J., Kim, D.H., Nam, B.Y., Kang, H.Y., Chang, T.I., Park, J.T., Han, S.H., et al. (2012). Apoptosis occurs differentially according to glomerular size in diabetic kidney disease. Nephrol. Dial. Transplant. *27*, 259–266.

11. Tikoo, K., Singh, K., Kabra, D., Sharma, V., and Gaikwad, A. (2008). Change in histone H3 phosphorylation, MAP kinase p38, SIR 2 and p53 expression by resveratrol in preventing streptozotocin induced type I diabetic nephropathy. Free Radic. Res. *42*, 397–404.

12. Peng, J., Li, X., Zhang, D., Chen, J.K., Su, Y., Smith, S.B., and Dong, Z. (2015). Hyperglycemia, p53, and mitochondrial pathway of apoptosis are involved in the susceptibility of diabetic models to ischemic acute kidney injury. Kidney Int. *87*, 137–150.

13. Deshpande, S.D., Putta, S., Wang, M., Lai, J.Y., Bitzer, M., Nelson, R.G., Lanting, L.L., Kato, M., and Natarajan, R. (2013). Transforming growth factor-β-induced cross talk between p53 and a microRNA in the pathogenesis of diabetic nephropathy. Diabetes *62*, 3151–3162.

14. Hoshino, A., Ariyoshi, M., Okawa, Y., Kaimoto, S., Uchihashi, M., Fukai, K., Iwai-Kanai, E., Ikeda, K., Ueyama, T., Ogata, T., and Matoba, S. (2014). Inhibition of p53 preserves Parkin-mediated mitophagy and pancreatic β-cell function in diabetes. Proc. Natl. Acad. Sci. USA *111*, 3116–3121.

15. Li, P., Zhang, X., Wang, L., Du, L., Yang, Y., Liu, T., Li, C., and Wang, C. (2017). lncRNA HOTAIR Contributes to 5FU Resistance through Suppressing miR-218 and Activating NF-κB/TS Signaling in Colorectal Cancer. Mol. Ther. Nucleic Acids *8*, 356–369.

16. Sun, C.C., Zhang, L., Li, G., Li, S.J., Chen, Z.L., Fu, Y.F., Gong, F.Y., Bai, T., Zhang, D.Y., Wu, Q.M., and Li, D.J. (2017). The lncRNA PDIA3P Interacts with miR-185-5p to Modulate Oral Squamous Cell Carcinoma Progression by Targeting Cyclin D2. Mol. Ther. Nucleic Acids *9*, 100–110.

17. Fu, Q., Qin, Z., Zhang, L., Lyu, D., Tang, Q., Yin, H., Chen, Z., and Yao, K. (2017). A New Long Noncoding RNA ALB Regulates Autophagy by Enhancing the

Transformation of LC3BI to LC3BII during Human Lens Development. Mol. Ther. Nucleic Acids *9*, 207–217.

18. Feng, L., Shi, L., Lu, Y.F., Wang, B., Tang, T., Fu, W.M., He, W., Li, G., and Zhang, J.F. (2018). Linc-ROR Promotes Osteogenic Differentiation of Mesenchymal Stem Cells by Functioning as a Competing Endogenous RNA for miR-138 and miR-145. Mol. Ther. Nucleic Acids *11*, 345–353.
19. Lv, L., Li, T., Li, X., Xu, C., Liu, Q., Jiang, H., Li, Y., Liu, Y., Yan, H., Huang, Q., et al. (2018). The lncRNA Plscr4 Controls Cardiac Hypertrophy by Regulating miR-214. Mol. Ther. Nucleic Acids *10*, 387–397.
20. Chung, A.C., Yu, X., and Lan, H.Y. (2013). MicroRNA and nephropathy: emerging concepts. Int. J. Nephrol. Renovasc. Dis. *6*, 169–179.
21. Lorenzen, J.M., Haller, H., and Thum, T. (2011). MicroRNAs as mediators and therapeutic targets in chronic kidney disease. Nat. Rev. Nephrol. *7*, 286–294.
22. Zhou, Q., Huang, X.R., Yu, J., Yu, X., and Lan, H.Y. (2015). Long Noncoding RNA Arid2-IR Is a Novel Therapeutic Target for Renal Inflammation. Mol. Ther. *23*, 1034–1043.
23. Li, Y., Wen, X., Wang, L., Sun, X., Ma, H., Fu, Z., and Li, L. (2017). lncRNA ZEB1-AS1 predicts unfavorable prognosis in gastric cancer. Surg. Oncol. *26*, 527–534.
24. Su, W., Xu, M., Chen, X., Chen, N., Gong, J., Nie, L., Li, L., Li, X., Zhang, M., and Zhou, Q. (2017). Long noncoding RNA ZEB1-AS1 epigenetically regulates the expressions of ZEB1 and downstream molecules in prostate cancer. Mol. Cancer *16*, 142.
25. Putta, S., Lanting, L., Sun, G., Lawson, G., Kato, M., and Natarajan, R. (2012). Inhibiting microRNA-192 ameliorates renal fibrosis in diabetic nephropathy. J. Am. Soc. Nephrol. *23*, 458–469.
26. Xie, H., Xue, J.D., Chao, F., Jin, Y.F., and Fu, Q. (2016). Long non-coding RNA-H19 antagonism protects against renal fibrosis. Oncotarget *7*, 51473–51481.
27. Wang, M., Yao, D., Wang, S., Yan, Q., and Lu, W. (2016). Long non-coding RNA ENSMUST00000147869 protects mesangial cells from proliferation and fibrosis induced by diabetic nephropathy. Endocrine *54*, 81–92.
28. Zhang, K., Han, X., Zhang, Z., Zheng, L., Hu, Z., Yao, Q., Cui, H., Shu, G., Si, M., Li, C., et al. (2017). The liver-enriched lnc-LFAR1 promotes liver fibrosis by activating TGFβ and Notch pathways. Nat. Commun. *8*, 144.
29. Zhou, Q., Chung, A.C., Huang, X.R., Dong, Y., Yu, X., and Lan, H.Y. (2014). Identification of novel long noncoding RNAs associated with TGF-β/Smad3-mediated renal inflammation and fibrosis by RNA sequencing. Am. J. Pathol. *184*, 409–417.
30. Liu, C., and Lin, J. (2016). Long noncoding RNA ZEB1-AS1 acts as an oncogene in osteosarcoma by epigenetically activating ZEB1. Am. J. Transl. Res. *8*, 4095–4105.
31. Kato, M., Arce, L., Wang, M., Putta, S., Lanting, L., and Natarajan, R. (2011). A microRNA circuit mediates transforming growth factor-β1 autoregulation in renal glomerular mesangial cells. Kidney Int. *80*, 358–368.
32. Rasouly, H.M., Kumar, S., Chan, S., Pisarek-Horowitz, A., Sharma, R., Xi, Q.J., Nishizaki, Y., Higashi, Y., Salant, D.J., Maas, R.L., and Lu, W. (2016). Loss of Zeb2 in mesenchyme-derived nephrons causes primary glomerulocystic disease. Kidney Int. *90*, 1262–1273.
33. Thienpont, L.M., Van Landuyt, K.G., Stöckl, D., and De Leenheer, A.P. (1995). Candidate reference method for determining serum creatinine by isocratic HPLC: validation with isotope dilution gas chromatography-mass spectrometry and application for accuracy assessment of routine test kits. Clin. Chem. *41*, 995–1003.
34. Zhan, M., Usman, I.M., Sun, L., and Kanwar, Y.S. (2015). Disruption of renal tubular mitochondrial quality control by Myo-inositol oxygenase in diabetic kidney disease. J. Am. Soc. Nephrol. *26*, 1304–1321.
35. Zhang, D., Pan, J., Xiang, X., Liu, Y., Dong, G., Livingston, M.J., Chen, J.K., Yin, X.M., and Dong, Z. (2017). Protein Kinase Cδ Suppresses Autophagy to Induce Kidney Cell Apoptosis in Cisplatin Nephrotoxicity. J. Am. Soc. Nephrol. *28*, 1131–1144.
36. Zhang, D., Sun, L., Xian, W., Liu, F., Ling, G., Xiao, L., Liu, Y., Peng, Y., Haruna, Y., and Kanwar, Y.S. (2010). Low-dose paclitaxel ameliorates renal fibrosis in rat UUO model by inhibition of TGF-beta/Smad activity. Lab. Invest. *90*, 436–447.
37. Zhang, L., Xu, X., Yang, R., Chen, J., Wang, S., Yang, J., Xiang, X., He, Z., Zhao, Y., Dong, Z., and Zhang, D. (2015). Paclitaxel attenuates renal interstitial fibroblast activation and interstitial fibrosis by inhibiting STAT3 signaling. Drug Des. Devel. Ther. *9*, 2139–2148.
38. Sun, L., Zhang, D., Liu, F., Xiang, X., Ling, G., Xiao, L., Liu, Y., Zhu, X., Zhan, M., Yang, Y., et al. (2011). Low-dose paclitaxel ameliorates fibrosis in the remnant kidney model by down-regulating miR-192. J. Pathol. *225*, 364–377.
39. Wang, J., Li, H., Qiu, S., Dong, Z., Xiang, X., and Zhang, D. (2017). MBD2 upregulates miR-301a-5p to induce kidney cell apoptosis during vancomycin-induced AKI. Cell Death Dis. *8*, e3120.